J Mater Sci (2020) 55:10910–10921

Polymers & biopolymers

Dual thermo-responsive amphiphilic alternating copolymers: one-pot synthesis and the temperature-induced self-assembly

Zi-Kun Rao[1], Hai-liang Ni[2], Yu Liu[1,*], Yang Li[1], Hong-Yu Zhu[1], and Jian-Yuan Hao[1,*]

[1] School of Materials and Energy, University of Electronic Science and Technology of China, No. 4 Block 2, North Jian'she Road, Chengdu 610054, China
[2] College of Chemistry and Materials Science, Sichuan Normal University, Chengdu, China

Received: 11 February 2020
Accepted: 29 April 2020
Published online: 11 May 2020

ABSTRACT

Synthesis and self-assembly of stimuli-responsive amphiphilic alternating copolymers (AAC) are an emerging land of tremendous possibilities. Herein, by combining backbone polyethylene glycol (PEG) with pendent oligo-polyglycol simultaneously, two alternating LCST segments are knitted through enzymatic synthesis, giving a series of alternating poly[(PEG400-a-succinic acid)-co-(-diol(3EG)-a-succinic acid)] (PPSDS) for the first time. All the PPSDSs show only one-step sharp temperature responsiveness in transmittance–temperature curve owing to stabilization effect of PEG400. The cloud points can be linearly controlled by simply adjusting the feeding ratio of PEG400/diol-3EG. Referring to published works and ^{1}H-NMR spectra in D_2O, all the obtained AAC formed penetrable nanovesicles under 4 °C. The TEM and ^{1}H-NMR results confirmed that when heated to 18 °C, PPSDS of "9/1" transformed from nanovesicles to large-compound micelles due to large hydrophobic volume, while other PPSDS of "8/2, 7/3, 6/4" retained the vesicle structures, except that the hydrophilic layer turned from PEG400 + diol(3EG) to PEG400 alone, leading to the size reduction. The temperature-controlled size "expansion and contraction" of nanovesicles was unique for AAC, which was potentially good for enhancing loading rate. Further heating above cloud point resulted in the destruction of nanostructures and irregular intermolecular aggregations. The first reported dual temperature-responsive AAC was innovative in structure design, providing a potential opportunity for the design and synthesis of controllable self-assemble structures and smart biomacromolecules in biomedical applications.

Co-first author: Zi-Kun Rao, Hai-liang Ni.

Address correspondence to E-mail: poly1634@hotmail.com; jyhao@uestc.edu.cn

https://doi.org/10.1007/s10853-020-04747-8

Introduction

In the past decades of years, stimuli-responsive polymers have attracted wide attention in the field of "smart" materials due to the capability of changing physiochemical properties in respond to external stimuli. Common external stimuli include temperature, electromagnetic radiation, pH values and some small molecules like glucose, which usually induce the changes of stimuli-responsive polymers in color, morphologies or phases [1]. Due to the convenience in temperature control, thermo-responsive polymers have become a hotspot and been widely applied in such fields as drug delivery system, tissue engineering and gene transfection [2–6]. Especially for the thermo-responsive drug delivery system, it is promising to improve the treatment efficacy of hyperthermia which could effectively destroy tumor cell while reducing damages to normal cells [7, 8]. Solubility of these polymers in water generally changes with increasing temperature; those dissolve under low temperature and precipitate under high temperature are named as LCST polymers; otherwise, those precipitate under low temperature and dissolve under high temperature are UCST polymers. Usually, it is preferred that drugs or agents are loaded into nanocarriers under mild temperature and released under body or higher temperature [9–11], which made LCST polymers much more prevailing in thermo-responsive materials.

Poly(N-isopropylacrylamide) (PNIPAAm)-based polymers are the most widely studied LCST materials with cloud point (32 °C) close to body temperature. Meanwhile, when combined with other polymers, peptides, liposomes or proteins, targeting delivery and drug-controlled release can be significantly improved [12, 13]. For instance, the semi-interpenetrating network structures of PNIPAAm can raise the cloud point (T_{cp}) up to 41 °C [14]. Combining PNIPAAm with polystyrene will give temperature-responsive nanocarriers with core–shell structures in water, which is helpful for the delivery of hydrophobic drugs in aqueous environment [15, 16]. The oligoethylene glycol (OEG)-grafted polymers are another kind of LCST materials, especially the OEG grafted methacrylate (OEGMA) and the derivatives, whose T_{cp}s can be adjusted by changing the lengths or end groups of pendent OEG [17]. Changing the ratios of OEGMA monomers of different side chain lengths can also precisely adjust the T_{cp} of resultant copolymers, and the huge hysteresis in PNIPAAm polymers between heating and cooling curves can be avoided in OEGMA polymers [18]. However, both of them are undegradable in backbones, which undermined their biocompatibility and biosafety.

The polycarbonates bearing pendent OEG were biodegradable while maintaining fast temperature responsiveness [19, 20]. However, like the above PNIPAAm or POEGMA, the homopolymers in water could only become random coils under low temperature. Introduction of hydrophobic segments could induce apparent phase separation, thus promoting the formation of nanospheres in aqueous solution [19, 21], but this method would limit the T_{cp} below that of hydrophilic homo-polycarbonates; plus the cumbersome preparation steps of modified carbonate monomers, some simple methods are needed to obtain LCST polyesters with innovative structures and controllable T_{cp}s. Presently, the traditional polymerization methods are usually not versatile enough to allow incorporation of diverse comonomers and to modify crucial properties like hydrophobicity of polyester products [22]. On the other hand, abundant of multifunctional polyesters have been prepared by lipase catalysts over the past two decades [23, 24]. The facile reaction conditions, high enantio-/chemo-/regio-selectivity and few side reactions in enzymatic polymerization [25] made it a convenient, green and controllable route to functional polyesters.

To the best of our knowledge, no researches referring to enzymatic synthesis of T_{cp} controllable polyesters have been reported. Meanwhile, lipase has shown high efficiency in catalyzing the polymerizations among various kinds of diols and diesters, giving alternating structures. Therefore, it is promising in preparing "smart" amphiphilic alternating copolymers (AAC) which is hard to be synthesized by chemical catalysis [26]. Since smart AAC has shown high tendency in replacing traditional smart polymers [27], we for the first time try to explore the enzymatic synthesis of T_{cp} controllable amphiphilic alternating polyesters with PEG segments on both backbones and side chains (Scheme 2). Monomer reactivity in enzymatic synthesis was studied in detail. In addition, as the dual temperature responsiveness has been reported in block copolymers with two LCST parts, it is interesting to investigate the

temperature-dependent self-assembly of these potential dual temperature-responsive polyesters knitted by two LCST alternating segments in random sequences. This fundamental research in novel LCST materials will be a pioneering step for developing much more multifunctional self-assembly system of AAC materials.

Experimental section

Materials

Trimethylolethane (TME) was purchased from Sigma-Aldrich (98%). The immobilized lipase B from Candida antarctica on acrylic resin (N435) was purchased from Sigma-Aldrich and dried under vacuum prior to polymerization. Diethyl carbonate (AR), diethylene glycol monomethyl ether (2mEG) (98%), triethylene glycol monomethyl (3mEG) (98%), tetraethylene glycol monomethyl ether (4mEG) (98%) were purchased from Tokyo Chemical Industry co., Ltd. Diphenyl ether (AR), p-Toluenesulfonic acid (98%), p-toluenesulfonyl chloride (AR), potassium hydroxide (KOH) (AR), benzaldehyde (AR), sodium hydride (NaH 60% in oil), PEG400 (AR), PEG800 (AR) were purchased from Chengdu Kelong Chemical Corp. (Chengdu, China). Diethyl malonate (C3), diethyl succinate (C4), diethyl adipate (C6), diethyl suberate (C8) and diethyl sebacate (C10) were all purchased from Tokyo Chemical Industry co., Ltd.

Synthesis of 3-(hydroxymethyl)-3-methyloxetane (HMO)

TME (240.3 g, 2 mol) and diethyl carbonate (290 ml, 2.4 mol) were charged into one flask. KOH (0.1 g) was added in as the catalyst. Under nitrogen atmosphere, temperature was raised up to 120 °C. After complete dissolution of TME into diethyl carbonate, the solution was refluxed under 120 °C for 4 h to remove the ethanol byproduct. Then, reaction was continued for another 6 h under 190 °C. Finally, temperature was naturally cooled to the temperature of 90 °C and distillation was conducted under vacuum (20 Pa); the fractions at 66 °C were collected as the target product. Yield: 70%. (Scheme 1) HMO ($CDCl_3$, 400 MHz): 1.3 ppm (s, 3H, CH_3C–); 3.7 ppm (d, 2H, –CCH_2OH); 4.4/4.6 ppm (d, 4H, OCH_2C–).

Synthesis of diol-2EG

Under the temperature of 120 °C, HMO (25.5 g, 0.25 mol) was slowly dropped into 2mEG (240.3 g, 2 mol) with concentrated sulfuric acid (0.4 g) as catalyst. After about 1 h when HMO was completely dropped into reaction mixture, the temperature was raised up to 135 °C and reaction mixture was vigorously stirred for 24 h. Then, distillation was conducted to collect the fraction (190 °C/150 °C) under the vacuum degree of 20 Pa. Finally, the crude product was redistilled to collect the fraction (180 °C/130 °C) as the pure product. Yield: 58%. (Scheme 1)

Synthesis of diol-3EG

Under the temperature of 130 °C, HMO (25.5 g, 0.25 mol) was slowly dropped into3mEG (328.4 g, 2 mol) with concentrated sulfuric acid (0.4 g) as catalyst. After about 1 h when HMO was completely dropped into reaction mixture, the temperature was raised up to 155 °C and reaction mixture was vigorously stirred for 28 h. Then, distillation was conducted to collect the fraction (220 °C/185 °C) under vacuum degree of 20 Pa. Finally, the crude product was redistilled to collect the fraction (210 °C/174 °C) as the pure product. Yield: 47%. (Scheme 1) Diol-2EG/Diol-3EG ($CDCl_3$, 400 MHz): 0.8 ppm (s, 3H, CH_3C–); 3.4 ppm (s, 3H, CH_3O–); 3.50–3.75 ppm (m, –OCH_2CH_2O–, –CCH_2O–).

Synthesis of diol-4EG

Synthesis of diol-4EG was divided into four steps (Scheme 1).

1. Synthesis of 5-hydroxymethyl-5-methyl-2-phenyl-1,3 -dioxane (HMPD)
   TME (24.7 g, 0.205 mol) and p-toluenesulfonic acid (1.2 g, 6.3 mmol) were first dissolved in THF (480 ml). Then, benzaldehyde (25 ml, 0.247 mol) was slowly dropped into the above solution under room temperature; the reaction was continued by vigorously stirring the mixture for 20 h before it was stopped by adding 0.38 ml of aqueous ammonium solution (28%) into reaction mixture for neutralization. Finally, the mixture was evaporated to remove the THF and extracted by CH_2Cl_2 and NaCl (aq) to collect the organic layer which was further dried over anhydrous $MgSO_4$. Yield: 78%. HMPD (DMSO, 400 MHz):

Scheme 1 Synthesis of diol-nEG monomers.

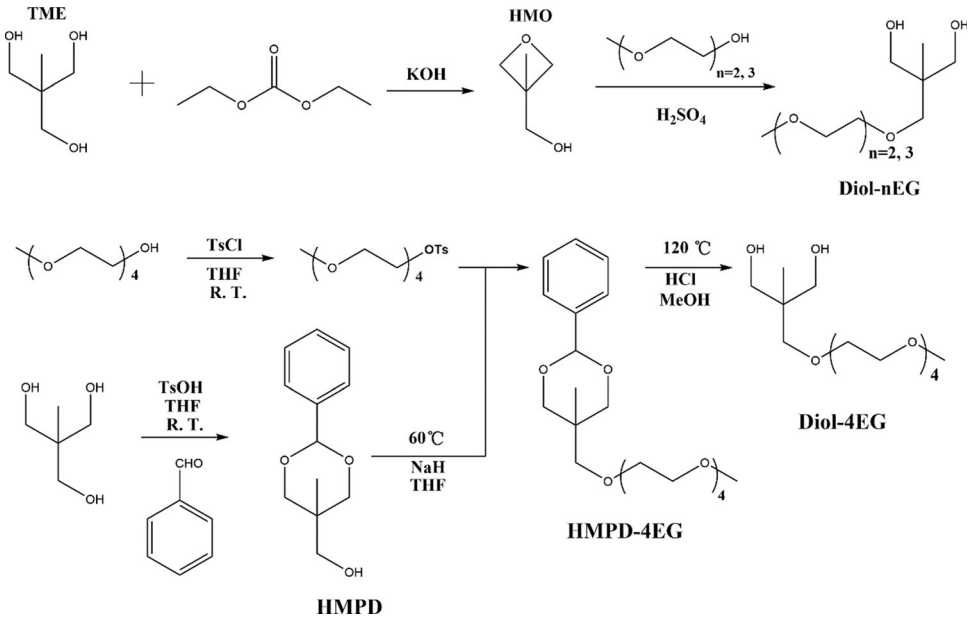

0.6/1.2 ppm (s, 3H, CH_3C–), 3.2/3.6 ppm (d, 2H, CH_2OH), 3.5–3.9 ppm (m, 4H, –OCH_2C–), 4.7 ppm (t, 1H, –OH), 5.3/5.4 ppm (s, 1H, –OCH–Ph), 7.30–7.44 ppm (m, 5H, Ph).

2. Tosylation of tetraethylene glycol monomethyl ether (4mEG-Ts)
   0.1 mol of tetraethylene glycol monomethyl ether was dissolved in 28 ml of hydroxide sodium solution (NaOH) (5 mol/L in water); the resultant mixture was put in ice bath. Then, p-toluenesulfonyl chloride (22.9 g, 0.12 mol) solution in anhydrous THF (120 ml) was dropped in; the reaction mixture was stirred vigorously for 8 h under ice bath before it was stirred for another 27 h. After that, the reaction mixture was extracted with CH_2Cl_2 and NaCl (aq) to collect the organic layer which was further dried over anhydrous $MgSO_4$. Yield: 97%. 4mEG-Ts ($CDCl_3$, 400 MHz): 2.42 ppm (s, 3H, CH_3-Ph); 3.3 ppm (s, 3H, CH_3O–); 3.5-3.8 ppm (m, 14H, –OCH_2CH_2O–), 4.3 ppm (t, 2H, CH_2–Ts–), 7.3 ppm (d, 2H, Ph), 7.8 ppm (d, 2H, Ph).
3. Synthesis of HMPD-4EG
   5.23 g (131 mmol) of NaH was charged into a three-necked flask under nitrogen atmosphere, and it was washed with 10 ml of THF for three times to remove the oils. Then, 14 ml of anhydrous N, N-dimethylformamide (DMF) and 70 ml of anhydrous THF were added in by injection. After 20.5 g of HMPD (98.5 mmol) was introduced into reaction flask, the mixture was stirred at 60 °C for 5 h under nitrogen atmosphere. After that, the 4mEG-Ts (19.98 g, 55.2 mmol) solution in anhydrous THF (10 ml) was slowly dropped into the reaction mixture which was stirred for another 14 h. The resultant mixture was extracted with CH_2Cl_2 and NaCl (aq) to collect the organic layer which was further dried over anhydrous $MgSO_4$. Finally, the crude mixture was purified by silica gel column chromatography with hexane/ethyl acetate (1/2, v/v) as eluent. Yield: 33%. HMPD-4EG ($CDCl_3$, 400 MHz): 0.8 ppm (s, 3H, CH_3C–), 3.37 ppm (s, 3H, CH_3O–), 3.5–4.1 ppm (m, 22H, –OCH_2CH_2O–, –CCH_2O–), 5.41 ppm (s, 1H, –OCH-Ph), 7.3–7.5 ppm (m, 5H, Ph).
4. Synthesis of diol-4EG
   HMPD-4EG (2 g, 5 mmol), methanol (10 ml) and dilute hydrochloric acid (10 ml, 5 mol/L) were charged into one flask. At the temperature of 110 °C, the reaction mixture was refluxed for 10 h and then naturally cooled down to room temperature. The resultant mixture was evaporated to remove residual methanol followed by adding in NaOH solution (5 mol/L) to adjust the pH value to 7.0. Finally, the mixture was extracted with CH_2Cl_2 and NaCl (aq) to collect the organic layer which was further dried over anhydrous $MgSO_4$.- Yield: 53%. Diol-4EG ($CDCl_3$, 400 MHz): 0.8 ppm (s, 3H, CH_3C–), 3.37 ppm (s, 3H, CH_3O–), 3.48–3.71 ppm (m, 22H, –OCH_2CH_2O–, –CCH_2-O–, –CCH_2OH)

Polymerization of alternating polyesters

3 mmol of diols (Diol-nEG or PEG400) and lipase N435 (10 wt.% of total monomers) were weighed and dried overnight under vacuum. 3 mmol of diesters was added into the above dried diols followed by the addition of diphenyl ether (200% by weight based on total monomers). Thereafter, the dried N435 was transferred into monomer mixtures. Under N_2 protection, the temperature was raised up to 80 °C and stirred for 2 h before the reduced pressure (10 mmHg) was applied for another 46 h. Polymerization was terminated by adding $CHCl_3$ to reaction mixture. After removing N435 particles through filter paper, the filtrates were concentrated and hexane was added in to induce precipitation. After it was washed with hexane for three times, the precipitation was dried at 40 °C under vacuum overnight.

Copolymerization of three-component LCST polyesters

High reactive diol-nEG, short PEG and diester monomers were chosen to be copolymerized by lipase catalysis. For the diol monomers, diol-nEG and short PEG were charged into the flask at the mole ratio of 9/1, 8/2, 7/3, 6/4; meanwhile, lipase N435 (10 wt.% of monomers) was weighed and charged into a tube. The diols and lipase were dried overnight under vacuum. Thereafter, diester ($n_{diol} = n_{diester}$) was added in followed by the addition of diphenyl ether (200% by weight based on total monomers). Then, the dried N435 was charged in, temperature was raised up to 80 °C, and the mixture was stirred for 12 h under nitrogen atmosphere. After that, reduced pressure (10 mmHg) was applied and copolymerization was continued for another 48 h. The reaction was terminated by adding $CHCl_3$ to reaction mixture. After removing N435 particles through filter paper, the filtrates were concentrated and hexane was added in to induce precipitation. After it was washed with hexane for three times, the precipitation was dried at 40 °C under vacuum overnight to obtain final products.

Characterization methods

^{1}H-NMR spectra. NMR spectra were recorded on a Varian-400-MR spectrometer at 400 MHz with deuterated chloroform ($CDCl_3$) or deuterium oxide (D_2O) as solvent. The chemical shifts (ppm) were referenced relative to tetramethylsilane (0.00 ppm). *GPC analysis.* Polymer average molecular weights and their distributions were monitored on a Waters Associates Model ALC/GPC 244 HPLC system (Milford, America) with Ultrastyragel Linear columns. The eluting solvent was THF at a flow rate of 1.0 mL/min at 35 °C. *Morphological Studies.* Morphological evaluation of the nanoparticles was performed using transmission electron microscopy (TEM) (ZEISS Libra 200 FE). *Dynamic light scattering analysis.* The size distributions of polymer aggregates in the aqueous phase were determined using dynamic light scattering (DLS) techniques with a Nanoseries (Malvern, UK) zetasizer with 90° instrument. Measurements were carried out at several temperature points. All the tests were conducted after 20 min of incubation. *Temperature-responsive behavior.* The optical transmittance of polyester aqueous solution (5 mg/ml) was measured with a UV–Vis spectrometer (Shimadzu: UV-2450); the 50% optical transmittance point was set as the cloud point (T_{cp}). Each sample was kept in the constant temperature oven for 5 min and immediately transferred to UV spectrometer to read the first optical transmittance value because the solution would soon become transparent with decreasing temperature (λ = 550 nm).

Results and discussion

Enzymatic synthesis and characterization of uniform AAC

In order to obtain LCST AAC with high molecular weights and fast temperature responsiveness, the uniform (or two-component) AAC were enzymatically prepared. Thereby, we could examine the reactivity and LCST behaviors in detail to select suitable monomers for the following three-component polymerization. The ^{1}H-NMR spectra of intermediate products and monomers for polymerization are presented in Supporting Information (Figure S1, Figure S2). The polymerization of PEG with diethyl succinate (C4) or diethyl adipate (C6) or diethyl suberate (C8) was performed at 80 °C for 48 h with lipase N435 as the catalyst. According to Table S1, all these poly(PEG-diacid) dissolved well in water, while only the most hydrophobic poly(PEG400-C8) and poly(PEG800-C10) showed apparent T_{cp} below 50 °C

(37 °C and 43 °C, respectively). Referring to the choice of monomers in the following three-component polymerization, PEG400 was chosen as one of the diol monomers due to its higher reactivity in polycondensation with diesters than PEG800, giving higher molecular weights with PDI close to 2.0.

Molecular weights and T_{cp} of uniform AAC between diol-nEG (n = 2, 3, 4) and diesters are presented in Fig. 1. The longer the pendent OEG, the lower the molecular weight, which was attributed to the steric hindrance of OEG chains. Therefore, the order of reactivity was "diol-2EG > diol-3EG > diol-4EG." Diol-4EG did not react with C4 diester due to the huge steric hindrance of long 4EG side chains to short diesters (C4). But it seemed to have some reactivity with longer C6 diester, giving low molecular weight and low PDI (1.5), which indicated that the hindrance effect did not work well on long-chain diesters.

It was also found that polyesters with longer OEG side chains and shorter diacid showed phase transition at higher temperature (e.g., T_{cp}: diol-3EG-C3 > diol-2EG-C3, diol-4EG-C6 > diol-3EG-C4, and diol-3EG-C3 > diol-3EG-C4) and responded faster to the temperature change, implying the hydrophilicity could enhance the temperature sensitivity and increase the T_{cp} point (Figure 1). Therefore, to ensure good temperature sensitivity, diols with longer pendent OEG and shorter-chain diesters were better choice (diol-4EG > diol-3EG > diol-2EG; C3 > C4 > others). However, compared with C3 diester, diesters

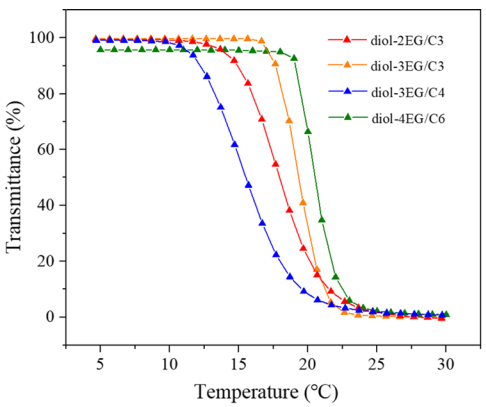

Copolymers	2EG-C3[b]	3EG-C3[b]	3EG-C4[b]	4EG-C4[b]	4EG-C6[b]
M_w[a]	7100	5700	2700	None	3300
PDI[a]	2.04	2.00	1.37	None	1.51
T_{cp}	18°C	20°C	16°C	\	21°C

a: based on GPC analysis (PS standard); b: nEG = diol-nEG; None: not react well.

Figure 1 Temperature-dependent transmittance of Poly(diol-nEG-diester) and the corresponding GPC results.

of C4, C6, C8 and C10 were more frequently applied in polymer biomaterials than C3 [28–30], which was probably due to their much weaker irritancy to living body than the strong acidic C3 acid during degradation. Considering the highest reactivity of C4 in polymerization with PEG400 (Table S1), C4 was the best diester monomer in the following enzymatic polymerization, and since diol-4EG could not react with C4 diester, diol-3EG was chosen as the other diol monomer instead.

It was worth mentioned that all the polyesters in Fig. 1 showed much lower T_{cp} than body temperature. Therefore, introduction of highly hydrophilic PEG was necessary to ensure that T_{cp} could be easily adjusted to body temperature. Meanwhile, the long flexible PEG segments were helpful in reducing the rigidity of alternating polyester chains knitted by dense ester bonds, which, to some extent, could promote intermolecular self-assembly of this amphiphilic alternating structure.

Enzymatic synthesis and the thermo-responsive behaviors of three-component random PPSDS

The synthesis and chemical structure of poly(-PEG400-a-succinic acid)-co-(diol(3EG)-a-succinic acid) (PPSDS) are shown in Scheme 2. ^{1}H-NMR spectra of these products at different diol ratios ($n_{diol-3EG}/n_{PEG400}$) are presented in Fig. 2; the characteristic signals of "h, f"(PEG400) at 4.20 ppm and 3.56 ppm, "b" (C4) at 2.67 ppm and "g, c, a" (diol-3EG) at 4.00 ppm, 3.38 ppm and 0.95 ppm confirmed the successful synthesis of PPSDS.

The proportion of different segments for these terpolymers was almost consistent with feed ratio according to ^{1}H-NMR spectra. The introduction of PEG400 into the backbone effectively increased the molecular weights of final products. As the ratio of PEG400 increased from 10 to 40%, the number-average molecular weights (M_n) was doubled with PDI increasing from 1.4 to 2.5. It was probably resulted from the solubilization effect of PEG400 segments, which restrained the precipitation of macromolecules (high polymerization degree) in nonpolar diphenyl ether.

As the proportion of PEG400 grew, T_{cp} increased from 26 °C to 41 °C, and temperature response speed was also accelerated (Fig. 3a). Unlike the "reel in" effects which resulted in irregular two-step transition

Scheme 2 Structure of poly(diol-3EG-co-PEG400-co-succinic acid).

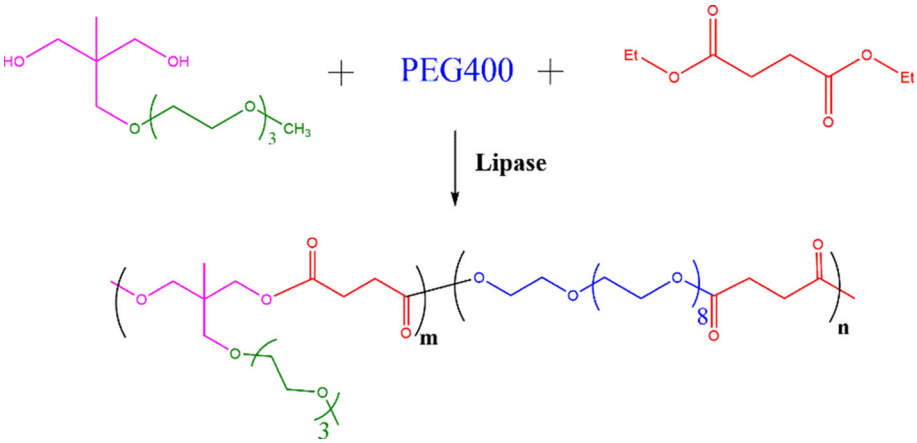

Figure 2 ^{1}H-NMR spectra of poly(diol-3EG-co-PEG400-co-succinic acid) (in $CDCl_3$) and the GPC results.

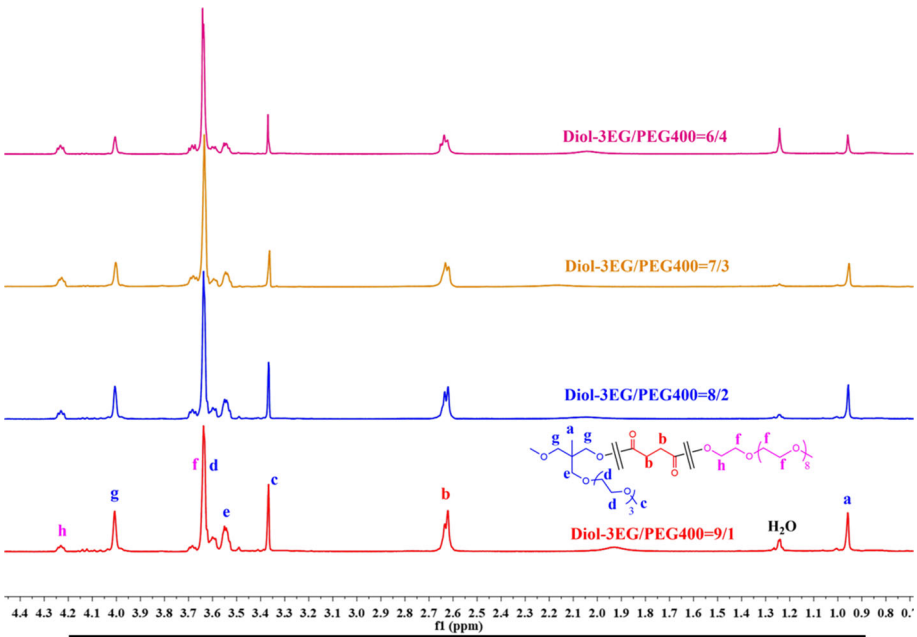

Feed Ratio (D/P/S)	Final ratio[a] (D/P/S)	M_n[b]	M_w[b]	PDI[b]	T_{cp}
9/ 1/ 10	8.6/ 1/ 10.2	4000	5700	1.42	26°C
8/ 2/ 10	8.1/ 2/ 10.2	6000	10800	1.80	32°C
7/ 3/ 10	7.2/ 3/ 10.5	7500	17900	2.39	36°C
6/ 4/ 10	6.7/ 4/ 10.6	8100	20300	2.51	41°C

D: Diol, P: PEG400, S: succinic acid; a: based on NMR spectrums ($CDCl_3$); b: GPC analysis (PS standard)

behaviors in random poly(2-ethoxyethyl vinyl ether-co-2-methoxyethyl vinyl ether) [31], terpolymers here all showed one-step sharp transition at proper temperature although they were composed of two kinds of LCST segments. It had been confirmed that amphiphilic alternating copolymers would readily assemble into nanodevices like micelles [21, 26] or vesicles [32, 33] in aqueous solution. However, when temperature was raised up high enough to make diol(3EG)-C4 segments hydrophobic, the long hydrophilic PEG chains could continue stabilizing the nanospheres. Therefore, reduction in optical transmittance was not found only if the temperature was high enough to induce the obvious dehydration of PEG segments in the backbone. The T_{cp} was almost linearly related to the ratio of PEG400 according to Fig. 3b. The formula could be given as Eq. 1, which

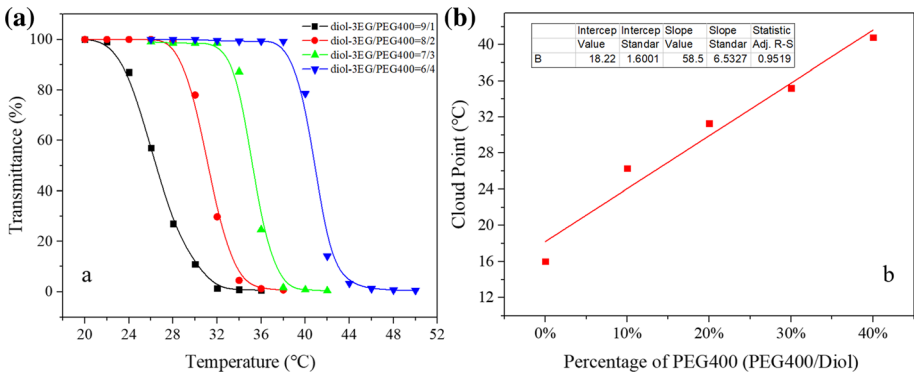

Figure 3 **a** Transmittance of different polyester aqueous solutions with temperature (5 mg/ml); **b** linear fitting between proportion of PEG400 and T_{cp} (5 mg/ml).

meant the T_{cp} could be easily regulated by changing the proportion of PEG400.

$$T_{cp} = 18.22 + 58.5 \times PEG400\% \ (R^2 = 0.95) \quad (1)$$

The influence of concentration on cloud points is displayed in Figure S3. The products with the ratio (diol-3EG/PEG400) of 8/2 were chosen as the sample in this evaluation. No apparent difference was found at the concentration of 8 mg/ml and 5 mg/ml, while response hysteretic occurred at 2 mg/ml, and the T_{cp} increased from 32 to 42 °C. It can be explained that higher concentration of polymer solution will benefit intermolecular aggregation, resulting in the lower phase transition temperature [19].

Self-assembly behaviors of PPSDS in aqueous solution

Self-assembly of alternating hydrophilic–hydrophobic polymers is an emerging topic. At present, it was found that AAC with flexible hydrophilic segments and large rigid hydrophobic segments tended to assemble into micelle [26, 27], while those with flexible hydrophilic and hydrophobic segments of comparable length or longer hydrophilic part could readily assemble into nanovesicles [32, 33]. Therefore, we inferred our amphiphilic alternating copolymer, with flexible backbones and short hydrophobic C4 segments, formed nanovesicles instead of micelles at low temperature (4 °C). When it was heated to 18 °C, diol(3EG)-C4 segment became dehydrated; the hydrophobic segment turned from sole C4 acid to diol(3EG)-C4 segments. Thereby, the hydrophobic parts were drastically augmented with the degree dependent on the ratio of diol-3EG. Copolymers of high PEG400 proportion could effectively keep the vesicle structures while those of low PEG400 proportion, with large hydrophobic segments, should aggregate into large-compound micelles [26].

TEM images of each polymer solution at 18 °C are presented in Fig. 4, which agreed with our conjecture. The PPSDS "9/1" with only 10% of PEG400 aggregated into irregular large-compound micelles with the size around 70 nm while other PPSDS with higher PEG400 content (8/2, 7/3, 6/4) all kept the vesicle structures with diameters ranging from 20 to 40 nm. But the average size of "7/3 and 6/4" was larger than that of "8/2." It was probably due to the higher hydrophilicity that led to larger water content inside nanovesicles.

^{1}H-NMR analysis in deuterium oxide (D_2O) was performed under various temperatures. PPSDS 8/2 was chosen as the research sample, and results are shown in Fig. 5. The signal of "CCH_2O" ("e") in diol-3EG was closer to the signal of methoxy("c") at all testing temperatures rather than the signals of "OCH_2CH_2O" ("f, d") as in $CDCl_3$. It was probably due to the reason that the end point methylene (e) was closer to end point methyl group (c) in terms of the chemical environment in aqueous solution. With temperature increasing, the gradual cleavage of hydrogen bonds resulted in left shift of the resonance toward low field. Meanwhile, all the signals in hydrophilic/hydrophobic segments appeared in the ^{1}H-NMR spectra in D_2O, which agreed with our conjecture that nanovesicles instead of micelles were formed in aqueous solution and the proportion of each unit based on integral areas is shown in Fig. 6a [The ratio of PEG400 was fixed to two tenths (2/10)]. DLS analysis showed similar results (Fig. 6b). The diameters reduced first and then grew during temperature heating. The size decreased at 18 °C owing to the dehydration of diol(3EG)-C4 segments, which induced the contraction of nanovesicles. Diameter growth at and above T_{cp} was resulted from the

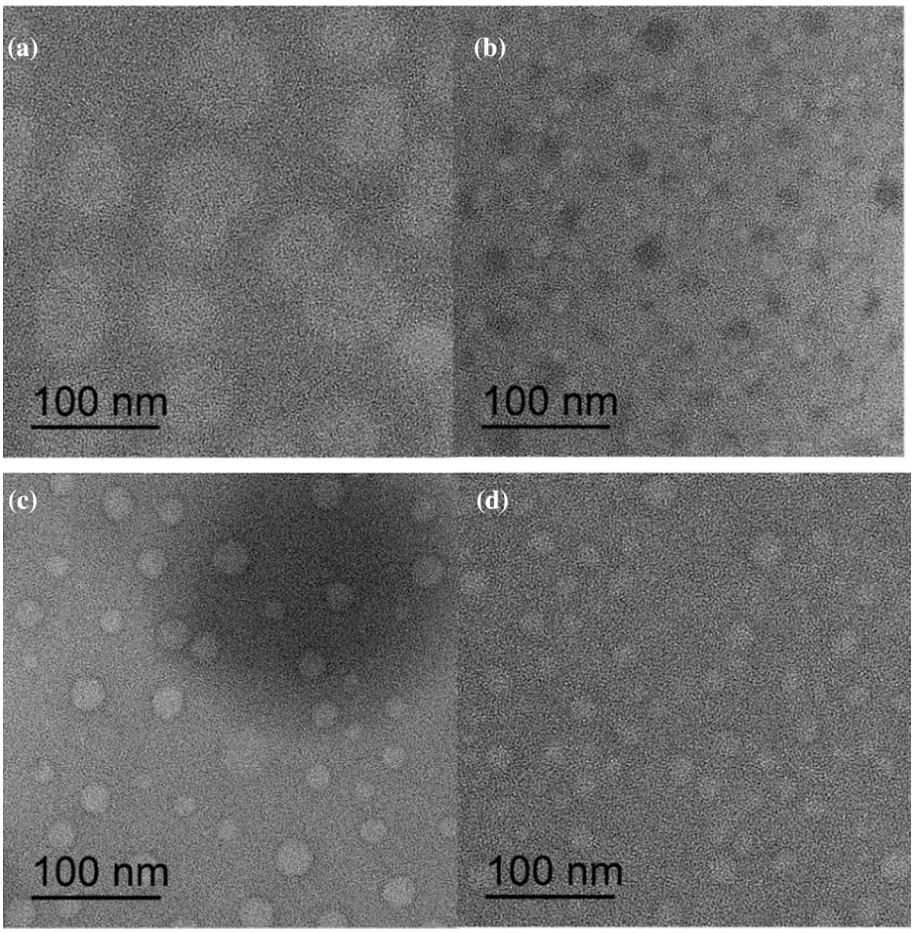

Figure 4 Morphologies of PPSDS in aqueous solution at 18 °C(5 mg/ml). **a** PPSDS 9/1; **b** PPSDS 8/2; **c** PPSDS 7/3; **d** PPSDS 6/4.

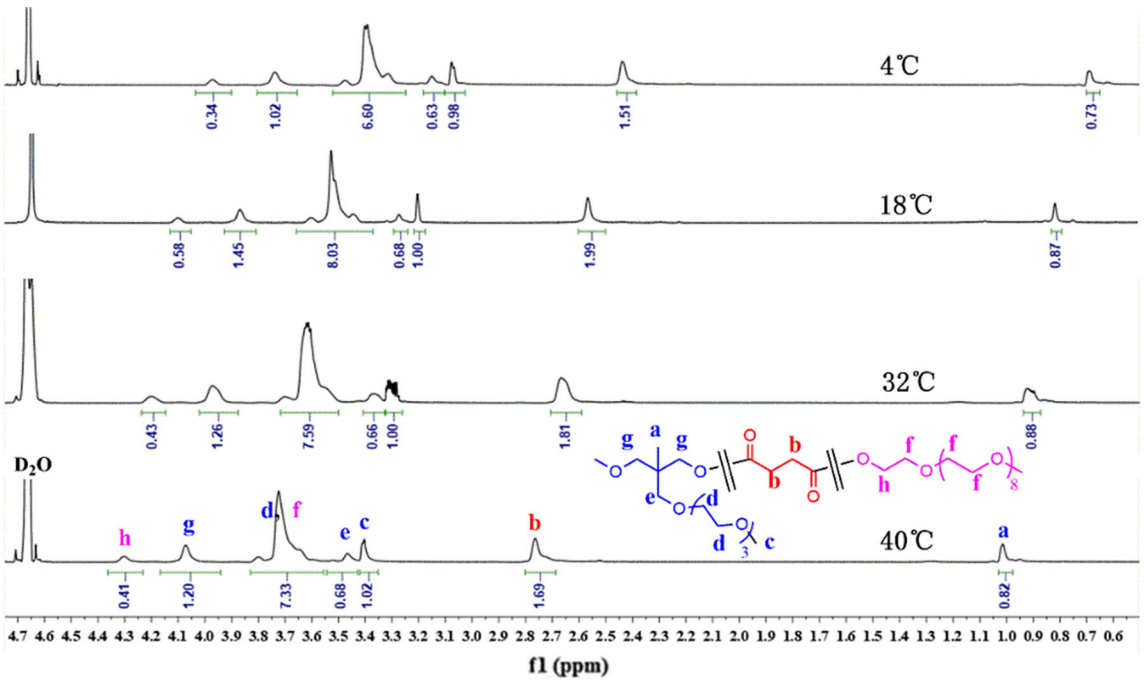

Figure 5 ^{1}H-NMR spectra under different temperatures in D_2O (PPSDS 8/2).

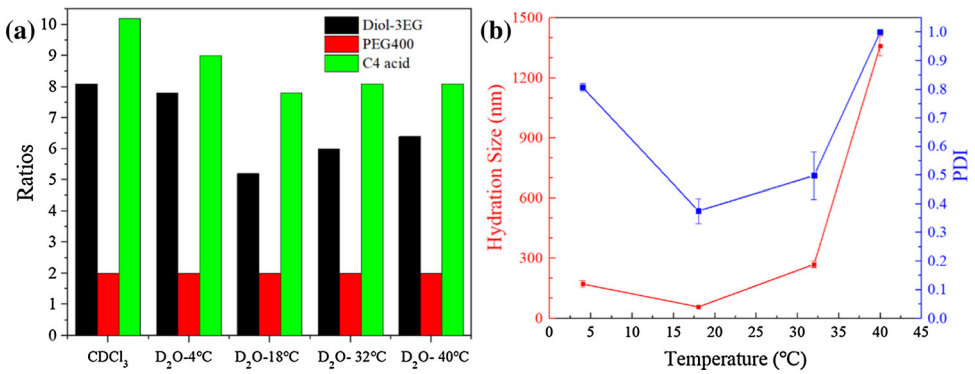

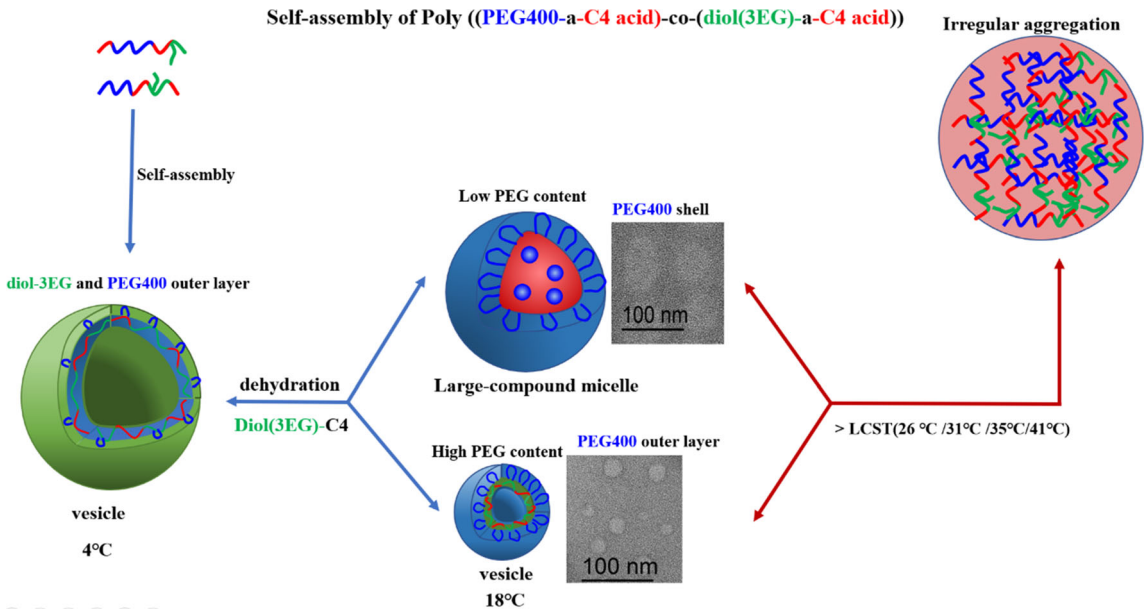

Figure 6 **a** Ratios of each monomer under different temperatures; **b** DLS results under different temperatures (PPSDS 8/2).

Figure 7 Illustration of dual thermo-responsive self-assembly behaviors of PPSDS.

dehydration of PEG chains and intermolecular aggregation.

According to the above analysis, the temperature-dependent self-assembly of PPSDS is presented in Fig. 7. Under low temperature, the bulgy vesicle with large diameters was formed. The dehydration of diol-3EG at 18 °C resulted in the phase transition into large-compound micelles for PPSDS 9/1 with low PEG400 content. But for PPSDS 8/2, 7/3, 6/4 with higher PEG400 content, nanovesicle scaffolds would be maintained, except that the size got smaller like a tightened net. The smaller diameters (about 50 nm) were advantageous for avoiding activating the immune response in circulation. In addition, because the vesicle scaffold was not broken, the nano-cargoes in the previous larger scaffolds could be maintained. Therefore, it was possible that "smaller" nanocarriers could wrap much more nano-cargoes by "controlled expansion and contraction" than they could by the "free packaging" in their small size, which was promising in increasing loading rate of nanocarriers. When temperature was further heated to or above cloud points, the nanovesicles began to collapse, and polymer chains irregularly aggregated into visible micron particles owing to the dehydration of PEG chains.

Conclusions

Lipase had shown good efficiency in catalyzing the preparation of T_{cp} controllable PPSDS in this research. Knitted by two alternating LCST segments, the obtained PPSDS showed two-step temperature-

dependent self-assembly behaviors. It could form bulgy nanovesicles under low temperature owing to the alternating amphiphilic structure. Apart from the PPSDS 9/1 with low PEG400 content, other PPSDS would transform into smaller vesicles when heated to 18 °C, which was helpful in avoiding immune response. The unique temperature-controlled expansion and contraction of nanovesicles need further investigation in the future works since it is of great potential to improve the problem of "loading rate" which greatly restrained the applications of nanocarriers. Interestingly, only one-step sharp phase transition was found in temperature–transmittance curves due to the stabilization effect of PEG400 in the backbone, giving only one T_{cp} for each product. By adjusting the ratio of PEG400, T_{cp} could be linearly controlled to target point ranging from 26 to 41 °C, which had covered all the important phase transition points like 32 °C for skin, 37 °C for body temperature and above 41 °C for hyperthermia. Meanwhile, all the components (PEG400, diacid with even chain length, TME) used in the polyesters have been proved to be biocompatible in previous works [30, 34, 35]. So, it is promising as a potential LCST biomedical material composed of biocompatible monomers and prepared by green methods. This work paved a new way in structure design, offering more possibilities for the combination of multifunctional groups into amphiphilic alternating structures.

Acknowledgements

This work was supported by the National Natural Sciences Fund of China (Nos. 31670979, 51273034), the Opening Project of the Key Laboratory of Advanced Technologies Materials, Ministry of Education (2016KLATM006) and Science and Technology Program of Sichuan Province (2018GZ0460 and 2019YFS0132).

Compliance with ethical standards

Conflict of interest The authors declare that they have no conflict of interest.

Electronic supplementary material: The online version of this article (https://doi.org/10.1007/s10853-020-04747-8) contains supplementary material, which is available to authorized users.

References

[1] Bawa P, Pillay V, Choonara YE et al (2009) Stimuli-responsive polymers and their applications in drug delivery. Biomed Mater 4:1–15

[2] Shimizu K, Fujita H, Nagamori E (2010) Oxygen plasma-treated thermoresponsive polymer surfaces for cell sheet engineering. Biotechnol Bioeng 106:303–310

[3] Twaites BR, Alarcon CDH, Lavigne M et al (2005) Thermoresponsive polymers as gene delivery vectors: cell viability, DNA transport and transfection studies. J Control Release 108:472–483

[4] Rao ZK, Chen ZM, Chen R et al (2019) Investigation of a novel thermogelling hydrogel for a versatility of drugs delivery. J Macromol Sci Part A Pure Appl Chem 56:26–33

[5] Stile RA, Healy KE (2001) Thermo-responsive peptide-modified hydrogels for tissue regeneration. Biomacromol 2:185–194

[6] Rao ZK, Chen R, Zhu HYu et al (2018) Carboxylic terminated thermo-responsive copolymer hydrogel and improvement in peptide release profile. Materials 11:338

[7] Koumenis C (2006) ER stress, hypoxia tolerance and tumor progression. Curr Mol Med 6:55–69

[8] Maxwell P, Dachs G, Gleadle J et al (1997) Hypoxia-inducible factor-1 modulates gene expression in solid tumors and influences both angiogenesis and tumor growth. PNAS Early Ed 94:8104–8109

[9] Qiu Y, Park K (2001) Environment-sensitive hydrogels for drug delivery. Adv Drug Deliv Rev 53:321–339

[10] Schmaljohann D (2006) Thermo- and pH-responsive polymers in drug delivery. Adv Drug Deliv Rev 58:1655–1670

[11] Fitzpatrick SD, Fitzpatrick LE, Thakur A et al (2012) Temperature-sensitive polymers for drug delivery. Expert Rev Med Devices 9:339–351

[12] Kelley EG, Albert JN, Sullivan MO, Epps TH III (2013) Stimuli-responsive copolymer solution and surface assemblies for biomedical applications. Chem Soc Rev 42:7057–7071

[13] Kono K, Henmi A, Yamashita H et al (1999) Improvement of temperature-sensitivity of poly(N-isopropylacrylamide)-modified liposomes. J Controlled Release 59:63–75

[14] Fu G, Soboyejo W (2010) Swelling and diffusion characteristics of modified poly (N-isopropylacrylamide) hydrogels. Mater Sci Eng, C 30:8–13

[15] Ballauff M, Lu Y (2007) "Smart" nanoparticles: preparation, characterization and applications. Polymer 48:1815–1823

[16] Picos-Corrales LA, Licea-Claveríe A, Arndt K-F (2014) Bisensitive core-shell nanohydrogels by e-Beam irradiation of micelles. React Funct Polym 75:31–40

[17] Vancoillie G, Frank D, Hoogenboom R (2014) Thermoresponsive poly (oligo ethylene glycol acrylates). Prog Polym Sci 39:1074–1095

[18] Lutz JF, Akdemir O, Hoth A (2006) Point by point comparison of twothermosensitive polymers exhibiting a similar LCST: is the age of poly(NIPAM) over? J Am Chem Soc 128:13046–130467

[19] Gu L, Qin Y, Gao Y et al (2013) Hydrophilic CO_2-based biodegradable polycarbonates: synthesis and rapid thermoresponsive behavior. J Polym Sci, Part A: Polym Chem 51:2834–2840

[20] Ajiro H, Takahashi Y, Akashi M (2012) Thermosensitive biodegradable homopolymer of trimethylene carbonate derivative at body temperature. Macromolecules 45:2668–2674

[21] Wang W, Ding J, Xiao C, Tang Z, Di Li J, Chen X, Zhuang X Chen (2011) Synthesis of amphiphilic alternating polyesters with oligo(ethylene glycol) side chains and potential use for sustained release drug delivery. Biomacromol 12:2466–2474

[22] Liu B, Zhang X, Chen Y, Yao Z, Yang Z, Gao D, Jiang Q, Liu J, Jiang Z (2015) Enzymatic synthesis of poly(ω-pentadecalactoneco-butylene-co-3,3′-dithiodipropionate) copolyesters and self-assembly of the PEGylated copolymer micelles as redox-responsive nanocarriers for doxorubicin delivery. Polym Chem 6:1997–2010

[23] Douka A, Vouyiouka S, Papaspyridi L, Papaspyrides CD (2018) A review on enzymatic polymerization to produce polycondensation polymers: the case of aliphatic polyesters, polyamides and polyesteramides. Prog Polym Sci 79:1–25

[24] Lu Y, Lv Q, Liu B, Liu J (2019) Immobilized Candida antarctica lipase B catalyzed synthesis of biodegradable polymers for biomedical applications. Biomater Sci 7:4963–4983

[25] Naolou T, Busse K, Kressler J (2010) Synthesis of well-defined graft copolymers by combination of enzymatic polycondensation and "click" chemistry. Biomacromol 11:3660–3667

[26] Xu Q, Li S, Yu C, Zhou Y (2019) Self-assembly of amphiphilic alternating copolymers. Chem Eur J 25:4255–4264

[27] Wu J, Xu B, Liu Z, Yao Y, Zhuang Q, Lin S (2019) The synthesis, self-assembly and pH-responsive fluorescence enhancement of an alternating amphiphilic copolymer with azobenzene pendants. Polym Chem 10:4025–4030

[28] Linko YY, Lamsa M, Wu X et al (1998) Biodegradable products by lipase biocatalysis. J Biotechnol 66:41–50

[29] Mahapatro A, Kalra B, Kumar A, Gross RA (2003) Lipase-catalyzed polycondensations: effect of substrates and solvent on chain formation, dispersity, and end-group structure. Biomacromol 4:544–551

[30] Korley JN, Yazdi S, McHugh K, Kirk J, Anderson J, Putnam D (2016) One-step synthesis, biodegradation and biocompatibility of polyesters based on the metabolic synthon, dihydroxyacetone. Biomaterials 98:41–52

[31] Okabe S, Seno K, Kanaoka S, Aoshima S, Shibayama M (2006) Micellization study on block and gradient copolymer aqueous solutions by DLS and SANS. Macromolecules 39:1592–1597

[32] Ding L, Li J, Jiang R, Wang L, Song W, Zhu L (2019) Noncovalently connected supramolecular metathesis graft copolymers: one-pot synthesis and self-assembly. Eur Polym J 112:670–677

[33] Li C, Chen C, Li S, Rasheed T, Huang P, Huang T, Zhang Y, Huang W, Zhou Y (2017) Self-assembly and functionalization of alternating copolymer vesicles. Polym Chem 8:4688–4695

[34] Taresco V, Creasey RG, Kennon J, Mantovani G, Alexander C, Burley JC, Garnett MC (2016) Variation in structure and properties of poly(glycerol adipate) via control of chain branching during enzymatic synthesis. Polymer 89:41–49

[35] Huang F, Cheng R, Meng F, Deng C, Zhong Z (2015) Micelles based on acid degradable poly (acetal urethane): preparation, pH-sensitivity, and triggered intracellular drug release. Biomacromol 16:2228–2236